



ISSN: 0067-2904

Ru⁺³, Rh⁺³, Pd⁺², Pt⁺⁴ and Au⁺³ Metal ions Complexes with Azo Derived from 4-Aminomethyl-cyclohexane carboxylic acid Synthesis, Characterization, Thermal Study and Antioxidant Activity

Isam Shaker Hamza¹, Rasha Khider Hussain Al-Daffay^{2*}, Saja S. Faris³, Abbas Ali Salih Al-Hamdani⁴

¹Department of Medical Laboratory Techniques, College of Health and Medical Techniques, Al-Esraa University

²Department of Chemistry, College of Science, University of Baghdad, Baghdad, Iraq

³Department of Chemistry, College of Education for Pure Science, Anbar University, Iraq

⁴Department of Chemistry, College of Science for Women, University of Baghdad, Baghdad, Iraq

Received: 23/10/2023

Accepted: 7/3/2024

Published: 30/3/2025

Abstract

The researchers aimed to develop a novel azo ligand as a continuation of their prior investigations. They synthesized the ligand, identified as N-(3-acetyl-2-hydroxy-5-methyl-phenyl)N-(4-carboxy-cyclohexylmethyl)-diazonium salt, and proceeded to synthesize a series of chelate complexes with Ru⁺³, Rh⁺³, Pd⁺², Pt⁺⁴, and Au⁺³ ions. Characterization of these compounds includes advanced techniques including elemental analysis, UV-Vis spectroscopy, FT-IR spectroscopy, LC-Mass spectrometry, NMR spectroscopy plus thermal analysis, conductivity measurements, magnetic quantification using TGA and DSC are used to further clarify the and synthesized complexes have been developed. Analysis revealed that the complexes formed with Ru⁺³, Rh⁺³, Pt⁺⁴, and Au⁺³ ions exhibited a 1:1 metal-ligand ratio and displayed octahedral geometry, with the exception of Pd⁺² and Au complexes, which displayed square planar geometry. The ligand itself was found to be tridentate (NOO) in nature. The thermal decomposition of some compounds using the TGA and DSC was studied and mass spectroscopy. The dye and the complexes were determined their ability to inhibit free radicals by measuring their ability as antioxidants using DPPH as a free radical and ascorbic acid as a standard substance, and determining the value of IC₅₀, as it was found that the ligand had a high ability to inhibit free radicals, and the ability to inhibit the complexes varied according to the value of IC₅₀. The results are as follows (Ascorbic acid > Au-complex > Pt-complex > Pd-complex > LH > Ru-complex

Keywords: Antioxidant, Azo dye, Au, Pt, Pd complexes, Mass spectra, thermal analysis

معقدات ايونات فلزات الذهب والبلاتين والبلاديوم والروديوم والروثينيوم مع الازو مشتق من 4-امينومثيل - سايكلووهكسان حامض الكاربوكسليك تحضير، تشخيص، دراسة حرارية وفعالية مضادات اكسدة

عصام شاكر حمزة¹، رشا خضر حسين الدفاعي²، سجي سعدون فارس³، عباس علي صالح الحمداني⁴
¹قسم تقنيات المختبرات الطبية، كلية التقنيات الصحية والطبية، جامعة الاسراء

*Email: rasha.khodair1105a@cs.w.uobaghdad.edu.iq

²قسم الكيمياء, كلية العلوم, جامعة بغداد, بغداد, العراق
³قسم الكيمياء كلية التربية للعلوم الصرفة, جامعة الانبار
⁴قسم الكيمياء, كلية العلوم للبنات, جامعة بغداد, بغداد, العراق

الخلاصة

اراد الباحثون تحضير ازو ليكاند جديدة كمتابعة لعملهم السابق. الليكاند (ن-3-استيل-2-هيدروكسي-5-مethyl-فينيل)-ن-4-كاربوكسي-سايلوكوهكسيل ميثيل-ملح الدايازونيوم), وتصنيع سلسلة من المعقدات المتناسقة لكل من ايونات الروثينيوم والروديوم والبلاديوم والبلاتينيوم والذهب. شخصت هذه المركبات باستخدام تقنيات متعددة تتضمن تحليل العناصر و تقنيات التحاليل الطيفية والتشخيصية (الاشعة فوق البنفسجية- المرئية والاشعة تحت الحمراء) ومطيافية الكتلة ومطيافية الرنين النووي المغناطيسي وتقنية التحليل الوزني الحراري والتوصيلية والحساسية المغناطيسية. وجد من خلال النتائج التحليلية ان معقدات الروثينيوم والروديوم والبلاديوم والبلاتينيوم والذهب تم تحضيرها بنسبة 1:1 (فلز : ليكاند) وان الشكل هندسي ثماني السطوح للمعقدات عدا معقدات الذهب والبلاديوم تكون ذات شكل مربع مستوي والليكاند متعادل ثلاثي السن يرتبط عن طريق (النتروجين والاكسجين والاكسجين). بعض المركبات درس تفككها حراريا بتقنية TGA DSC فضلاً عن اطياف الكتلة. استخدمت الصبغة والمعقدات المحضرة لتقدير قابليتها في تثبيط الجذور الحرة بواسطة قياس قابليتها كمضادات اكسدة باستخدام مادة (2,2-ثنائي فينيل-1-بكريلهايدرازين) كجذور حرة بوجود حامض الاسكوربيك كمادة قياسية وتقدير قيمة تركيز المادة الموافق للتثبيط النصفوي وقد وجد ان الليكاند تمتلك قابلية عالية في تثبيط الجذور الحرة كما ان القدرة التثبيطية للمعقدات تترتب حسب قيم C_{50} او كما يلي:
 Ascorbic acid > Au-complex > Pt-complex > Pd-complex > LH > Ru-complex

الكلمات المفتاحية : مضادات الاكسدة، اصباغ الازو، معقدات الذهب والبلاتين والبلاديوم، اطياف الكتلة والتحليل الحرارية

Introduction

Azo dyes currently dominate global dye production chemistry, with their relative industrial importance expected to potentially grow further in the future. They play a vital role in dye and printing market management [1]. Azo dyes constitute an important class of organic compounds characterized by the presence of at least one azo chromophore (-N=N-) which confers color upon the dye [2]. Depending on whether the R1 and R2 substituents are alkyl or aryl groups, azo compounds can be classified into two types [2]. First synthesized as model organic molecules, azo compounds continue to be manufactured at massive scales for the dye industry even today [1, 3]. Their widespread applications stem from desirable properties such as synthetic versatility, vivid hues, and excellent fastness characteristics. The azo is determined by the kind of substituents and where they are located on the aromatic ring. The ability of dyes to absorb electromagnetic energy in the visible region (400-700 nm) determines their hue[4]. A colored dye, according to Witt theory, needs both an auxochrome group and a chromophore group. Auxochromes increase the color of a colored molecule when added, whereas chromophores (such as nitro, azo, and quinoid groups) give color to the dye because they can absorb visible light. The current electronic theory has taken the place of Witt theory. This hypothesis states that color is the result of valence p electrons being excited by visible light (Murrell 1973) [5,6]. Azo compounds derive their core structure from the characteristic azo functional group (-N=N-) which links two organic substituents, such as symmetric/asymmetric or symmetric/non-symmetric alkyl or aryl radicals [7]. The colors imparted by azo dyes originate from contributions of the azo bonds themselves as well as any attached chromophores or autochromes [8-12]. Azo compounds are highly valued across diverse fields of chemical research due to the versatile functionalities that facilitate coordination complex formation with a wide range of metal ions [13]. These coordination

complexes exhibit diverse colors, high molar absorptivity and high thermal/photolytic stabilities. The current work aims to synthesize novel azo derivatives and investigate how alterations in substituents influence their metal binding and spectral properties. Different analysis techniques, including FT-IR, mass spectrometry, UV-Vis spectrum, $^1\text{H-NMR}$, and $^{13}\text{C-NMR}$, as well as thermal analysis, molar conductance, magnetic susceptibility, chloride content, FAA, and CHN elemental analysis, were used to characterize the produced complexes. Metal ions Ru^{+3} , Rh^{+3} , Pd^{+2} , Pt^{+4} and Au^{+3} Metal interacted in a 1:1 molar ratio with the azo ligand N-(3-Acetyl-2-hydroxy-5-methyl-phenyl)-N-(4-carboxy-cyclohexylmethyl)-diazonium, resulting in complexes with the formula $[\text{M}(\text{L})(\text{Cl})]\text{X}$, with $\text{X}=\text{Cl}$ for $\text{M}=\text{Au}^{+3}$ and $\text{X}=\text{O}$ for $\text{M}=\text{Pd}^{+2}$ with Square planer geometry, $[\text{M}(\text{L})(\text{H}_2\text{O})(\text{Cl})_2]$ for ($\text{M}^{+3}=\text{Rh}, \text{Ru}$) with octahedral geometry and $[\text{Pt}(\text{L})(\text{Cl})_3]$ with octahedral geometry. Since it was discovered that the ligand had a high ability to inhibit free radicals, and the ability to inhibit the complexes varied according to the value of IC_{50} , it was decided to measure the ability of the ligand and its complexes as antioxidants using DPPH as a free radical and ascorbic acid as a standard substance.

Materials and Methods

All reagents and starting materials were obtained from commercial suppliers Sigma Aldrich and Merck and used without further purification. Elemental analysis of carbon, hydrogen and nitrogen was carried out using a Euro vector EA3000 series elemental analyzer. After digestion, the metal ion content was determined gravimetrically and the relative metal oxides content was calculated. Molar conductivity measurements of the synthesized complexes (1×10^{-3} M solution in dimethylformamide) were carried out at room temperature using a WTW Conductometer Mass spectrometry was carried out on a Shimadzu QP-2010 Plus mass spectrometer operating in positive ionization mode to obtain molecular ion peak data was recorded on an FT-IR spectrometer. Furthermore, the UV-visible spectra of the complexes were obtained from the DMF solution using a Shimadzu UV-Vis 1800 Shimadzu spectrophotometer. The (^1H and $^{13}\text{C-NMR}$) spectra of the ligand in DMSO-d_6 were captured using a Bruker 300MHz. Thermalgravimetric analysis studies were carried out using the Perkin-Elmer Pyris Diamond TGA.

Synthesis of azo dye ligand: N-(3-Acetyl-2-hydroxy-5-methyl-phenyl)-N-(4-carboxy-cyclohexyl methyl)-diazonium

The synthesis of the azo ligand was performed in several steps. In the first step, 0.158 g (1 mmol) of 4-aminoethyl-cyclohexane carboxylic acid was dissolved in 10 mL of ethanol and 3 mL of concentrated hydrochloric acid and this solution was then cooled to 5°C by 0.158 g added on (1 mmol) of sodium nitrite in 10% solution under stirring performed Diazotization. Separately, 0.15 g (1 mmol) of 1-(2-hydroxy-5-methyl-phenyl)-ethanone was dissolved in ethanol and cooled. The diazotized acid solution prepared above was slowly added to this solution with stirring. This resulted in the formation of an insoluble black liquid, which was the target azo ligand. The precipitate was washed several times with a 1:1 mixture of ethanol and water to remove inactive precursors. Finally, it was dried to afford the pure azo ligand. The reaction scheme is described in Scheme 1. These multistep syntheses involving diazotization and coupling reactions yielded the desired azo-containing ligand. The $^1\text{H-NMR}$ spectra of the ligand in DMSO-d_6 and $^{13}\text{C-NMR}$ in Chloroform Figures 1 and 2, respectively show signals deal to contain the azo ligand. In the ^1H & $^{13}\text{C-NMR}$ revealed a peak at δ (3.66) ppm, which was ascribed to $\text{N}=\text{N}-\text{CH}_2$ chemical changes. The chemical shift of (CH_2-CH_2) protons on cyclohexane ring was ascribed to the peaks at δ (2.38, 2.45) ppm, the signals at (12.0) and (8.75) ppm were ascribed to the protons of (OH) carboxylic group and phenolic group respectively. The aromatic protons of benzene groups are attributed to the numerous peaks at δ (7.73–7.72) ppm, while in the $^{13}\text{C-NMR}$ shows signals in $\text{C}15= 19.55$,

C16= 25.24, C1,2,4,5= 34.12-34.14, C3,6 =44.28, C7= 53.75, C12= 127.64, C9= 128.47, C10= 133.97, C11= 140.88, C13= 155.27, C17= 173.45, C14 = 194.97, respectively[14-16].

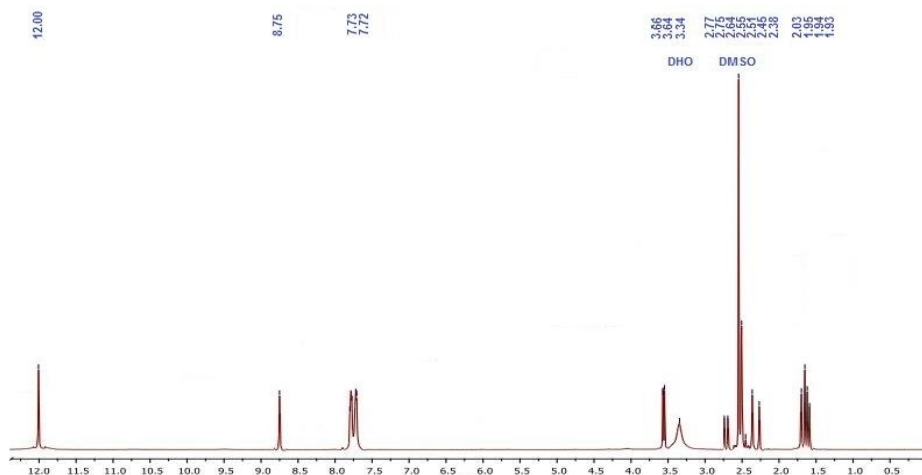


Figure 1: $^1\text{H-NMR}$ spectrum of ligand

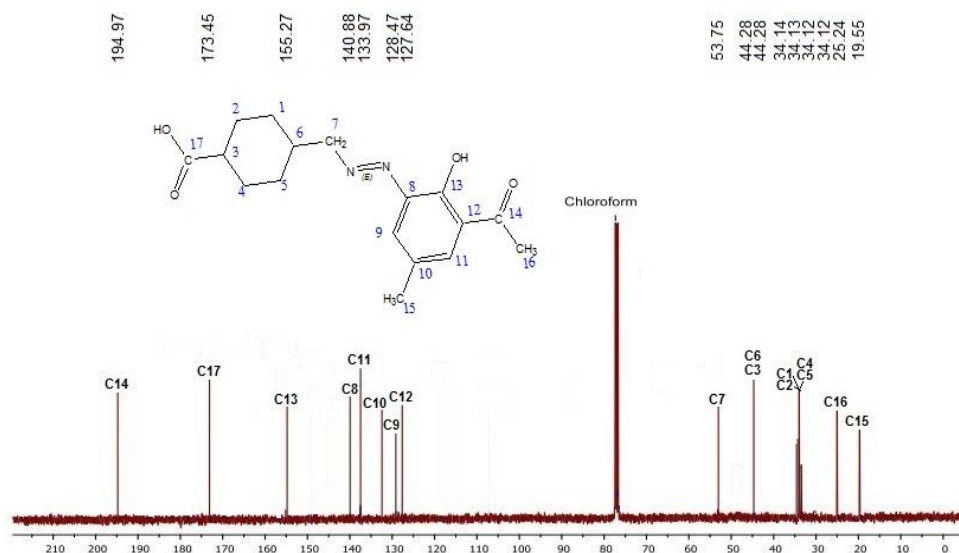
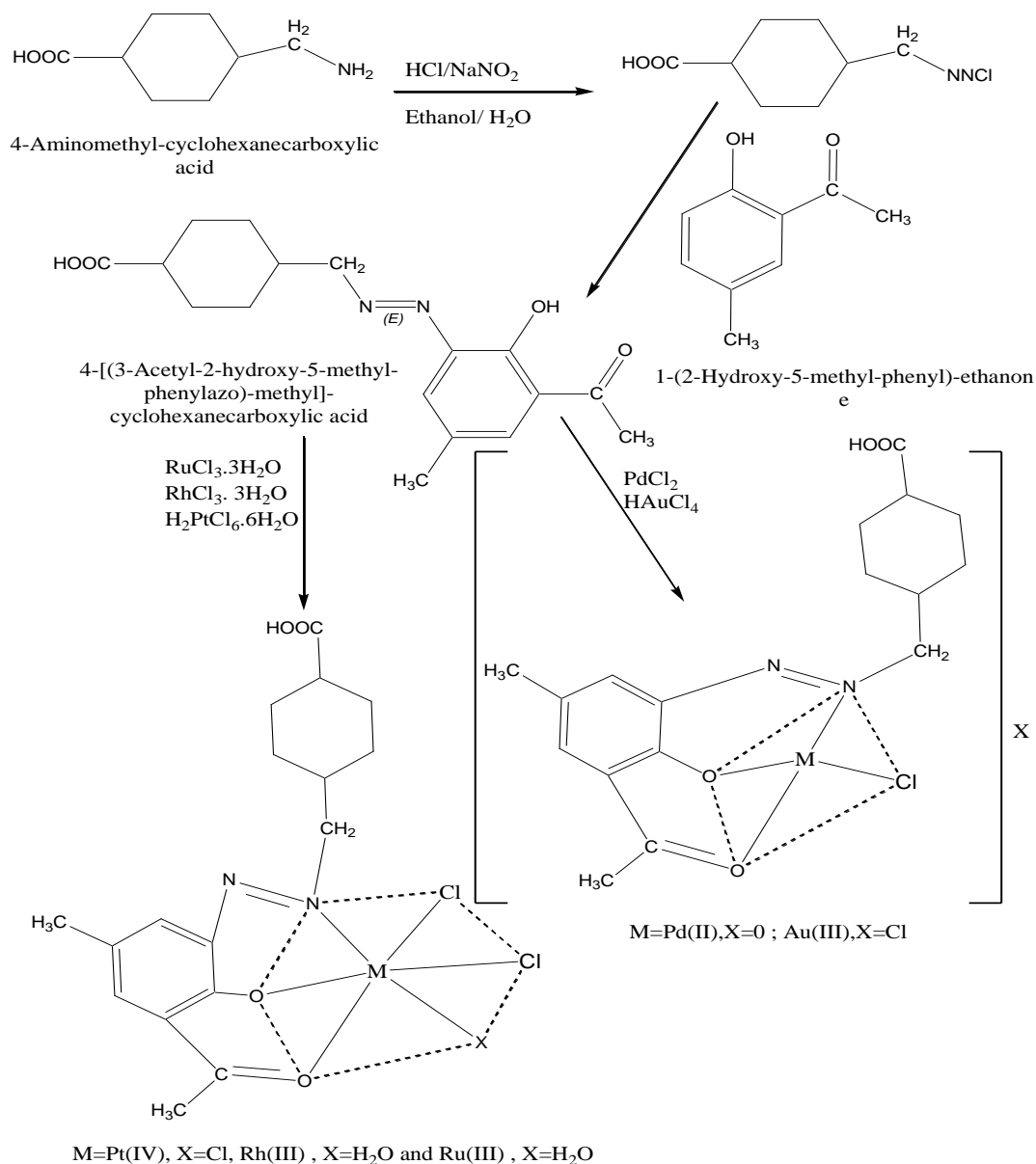


Figure 2: $^{13}\text{C-NMR}$ spectrum of ligand

Preparation of metallic complexes

Metal complexes of the synthesized azo ligand were prepared employing metal chloride salts of Ru^{+3} , Rh^{+3} , Pd^{+2} , Pt^{+4} , and Au^{+3} . For each complex, stoichiometric amounts of metal chloride and ligand were used in a 1:1 molar ratio. Specifically, 0.311 g $\text{RuCl}_3 \cdot 3\text{H}_2\text{O}$, 0.313 g $\text{RhCl}_3 \cdot 3\text{H}_2\text{O}$, 0.266 g PdCl_2 , 0.518 g $\text{H}_2\text{PtCl}_6 \cdot 6\text{H}_2\text{O}$ and 0.340 g HAuCl_4 (1 mmol each) were gradually added in a dropwise manner to 10 mL ethanolic solutions of the ligand (0.319 g, 1 mmol) under constant stirring. The molar ratio was chosen based on the coordination geometry expected between metal centers and multi-dentate azo ligand. The resulting solutions yielded metal complexes in high purity upon stirring overnight followed by crystallization. Extensive washing of the precipitates with ethanol ensured removal of unreacted reagents. This protocol employing slow addition and stoichiometric control facilitated efficient complexation between the hard acids (metal ions) and the chelating azo ligand. The combination was brought to between (60 and 70°C) over the course of two hours, cooled in an ice bath until precipitation started to form, and then permitted to stand overnight. To get rid of any unreacted components, the solid complexes were separated and washed with distilled water and a small amount of hot ethanol. Vacuum desiccators were then used to dry

the compounds. The ligand and its metal complexes' analytic and physical characteristics are included in Table 1 for convenience, Scheme 1. Synthesis of compounds.



Scheme 1: Synthesis of azo dye ligand and metal complexes

Results and discussion

The synthesized azo ligand (LH) presented as an amorphous fine orange powder upon isolation. Its non-crystalline nature indicates an irregular molecular packing, which was further supported by its variable solubility in different solvent systems. LH exhibited good solubility in polar aprotic solvents such as dimethylformamide (DMF) and dimethyl sulfoxide (DMSO), enabling spectroscopic characterization via solution studies. However, ethanol was found to be the most suitable solvent for recrystallization and obtaining high purity solid samples of LH. The resulting complexes of metallic ions and azo ligand were stable in the presence of air, and the analytic and physical characteristics are included in Table 1, the analysis results were compatible with theoretical calculated.

Table 1: Physical properties, analytical data of ligand and their complexes

Compound	M.wt	C Exp. Theo.	H Exp. Theo.	N Exp. Theo.	M Exp. Theo.	Cl Exp. Theo.	mp °C.	color
LH	318.37	65.07 64.13	7.11 6.97	7.77 8.80	-	-	188-190	orange
C ₁₇ H ₂₁ AuCl ₂ N ₂ O ₄	585	35.55 34.89	3.05 3.62	5.53 4.79	32.81 33.66	13.02 12.12	221-224 d	Light brown
C ₁₇ H ₂₁ ClN ₂ O ₄ Pd	459.23	45.21 44.46	3.84 4.61	7.44 6.10	22.99 23.17	7.26 7.72	284-287d	Dark brown
C ₁₇ H ₂₁ Cl ₃ N ₂ O ₄ Pt	618.80	33.50 33.00	4.05 3.42	5.18 4.53	32.22 31.53	16.55 17.19	277-280 d	brown
C ₁₇ H ₂₃ Cl ₂ N ₂ O ₅ Rh	509.19	41.05 40.10	5.16 4.55	6.08 5.50	20.88 20.21	13.22 13.93	288-290d	brown
C ₁₇ H ₂₃ Cl ₂ N ₂ O ₅ Ru	507.35	41.17 40.24	3.94 4.57	6.49 5.52	20.01 19.92	13.22 13.98	257-261 d	brown

Exp.: Experimental, **Theo.:** Theoretical, **d=** decompose

FT-IR spectroscopy

The infrared spectrum of the ligand showed multiple absorption bands (3459, 1451, 1671 and 3250 cm⁻¹) that could be attributed to the phenolic group, azo group, ketogenic and carboxylic carbonyl group, as well as other bands. From the Table 2 of IR spectra of all produced compounds revealed that the band of phenolic hydroxide was disappeared in the complexes that means the ligand coordinated through this group in all complexes, and the ketonic carbonyl and azo groups were shifted in the complexes and show new bands to (M-N, M-O and M-Cl) that means the azo-dye ligand connected to metal ion through three sites: the azo group's nitrogen site, oxygen of phenol group, and oxygen site of ketone group [17-20]. As a result, the ligand behaved as an N,O,O tridentate ligand in all complexes.

Table 2: The IR spectra bands (cm⁻¹) of compounds

Comp.	ν OH carboxylic	ν CO ketonic	ν (N=N)	Other bands
LH	3250	1671	1451	ν OH phenolic (3459)
[AuLCl]Cl	3259	1641	1466	ν M-N(511,469), ν M-O(429) ν M-Cl(380),
[PdLCl]	3244	1635	1463	ν M-N(480,466), ν M-O(427) ν M-Cl(381)
[RuL(H ₂ O)Cl ₂]	3246	1640	1441	ν M-(454,436), ν M-O(415) ν M-Cl(371), ν (H ₂ O) aqua(3456, 1633, 840,682)
[RhL(H ₂ O)Cl ₂]	3254	1658	1444	ν M-N(479,474), ν M-O(430), ν M-Cl(382) ν (H ₂ O) aqua(3450, 1613, 832,687)
[PtLCl ₃]	3257	1651	1445	ν M-N(462,444), ν M-O(413) ν M-Cl(392)

UV-Vis spectra, mass Spectrum, molar conductivity and magnetic susceptibility

The UV-Vis spectrum of the ligand showed multiple absorption peaks at 269, 310 and 350 nm that could be attributed to $\pi \rightarrow \pi^*$ and $n \rightarrow \pi^*$. The UV-Vis spectra of the Pd⁺² complex are shown in Table 3 and Figure 3, with peaks at 370 and 500 nm, 27027.0 and 20000 cm⁻¹, MLCT and ¹A_{1g} → ¹B_{1g}, respectively and absorption maxima at 310 nm attributable to the inter ligand. The Ru⁺³ complex's (Fig. 4) electronic spectra contained three absorption peaks. The peak at 499 is assigned to the (d-d) electronic transitions types ¹A_{1g} → ¹T_{1g}(G), whereas the peaks at 232, and 410 nm are attributed to the ligand and C.T., respectively. The peaks at 232 in the Rh⁺³ complex was attributed to the inter ligand, with the peak at 412 nm correlating to the C.T (M → L). electronic transitions and the peak at 499 nm being assigned to the ¹B_{2g} → ¹E_g transition, implying Octahedral. The Pt⁺⁴ complex's electronic spectra showed six peaks at 260, and 310 nm that correspond to the inter ligand, as well as a peak at 415 nm that was assigned to the C.T (M → L). Electronic spectra were useless due to the impossibility of d-d transitions, but the magnetic susceptibility of the Au⁺³ complex revealed the presence of diamagnetic moments and The Auric ion complex's electronic spectra showed two peaks at

434, and 600 nm that correspond to the $^1A_{1g} \rightarrow ^1B_{1g}$ and $^1A_{1g} \rightarrow ^1A_{2g}$, respectively. This conclusion really agrees well with other studies on square planer geometry [20-22]. The measured molar conductivity are (13.76, 9.21, 14.8 and 11.42) Λm ($S.cm^2.mol^{-1}$) non electrolyte for all complexes but Au-Complex 44.6 Λm ($S.cm^2.mol^{-1}$) electrolyte (1:1) [23, 24]. The magnetic measured was of the prepared Pd, Pt Au and Rh-complexes showed in Table 3, diamagnetic but Ru-Complex the magnetic value 1.77 B.M. respectively, This agreement with octahedral geometry for all complexes, the Pd and Au-complexes with square planer [25].

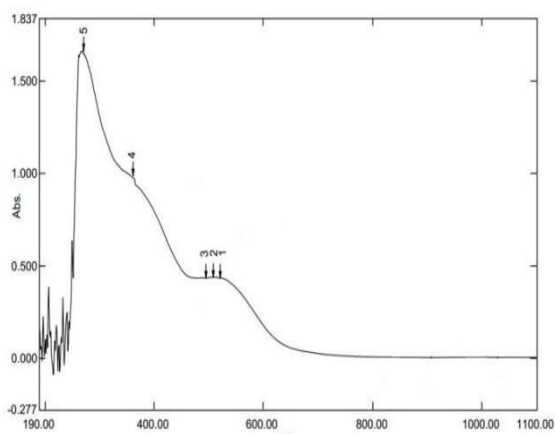


Figure 3: UV-Vis spectrum of Pd-complex

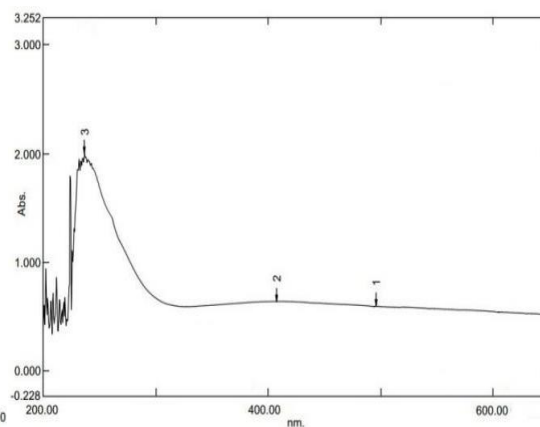


Figure 4: UV-Vis spectrum of Ru-complex

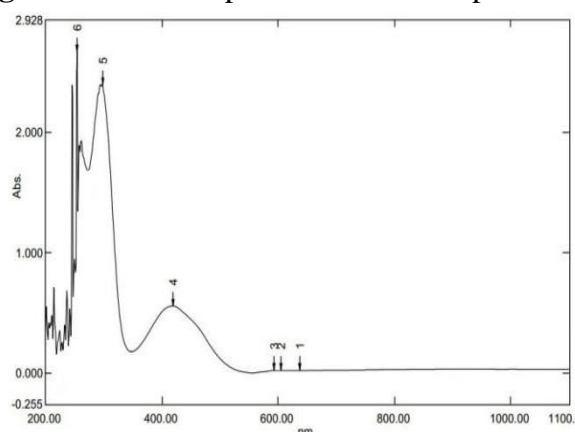


Figure 5: UV-Vis spectrum of Pt-complex

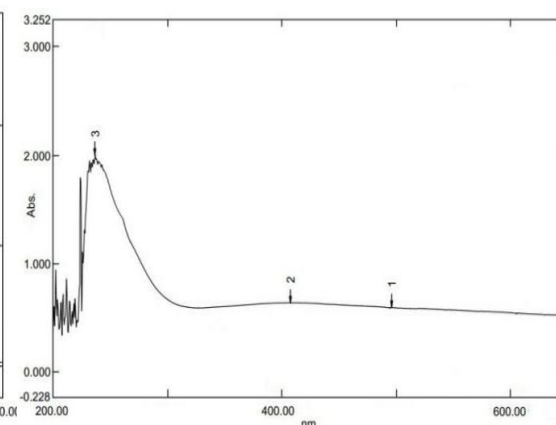


Figure 6: UV-Vis spectrum of Rh-complex

Table 3: Electronic spectral data of the compounds and molar conductivity in DMF (1×10^{-3} M)

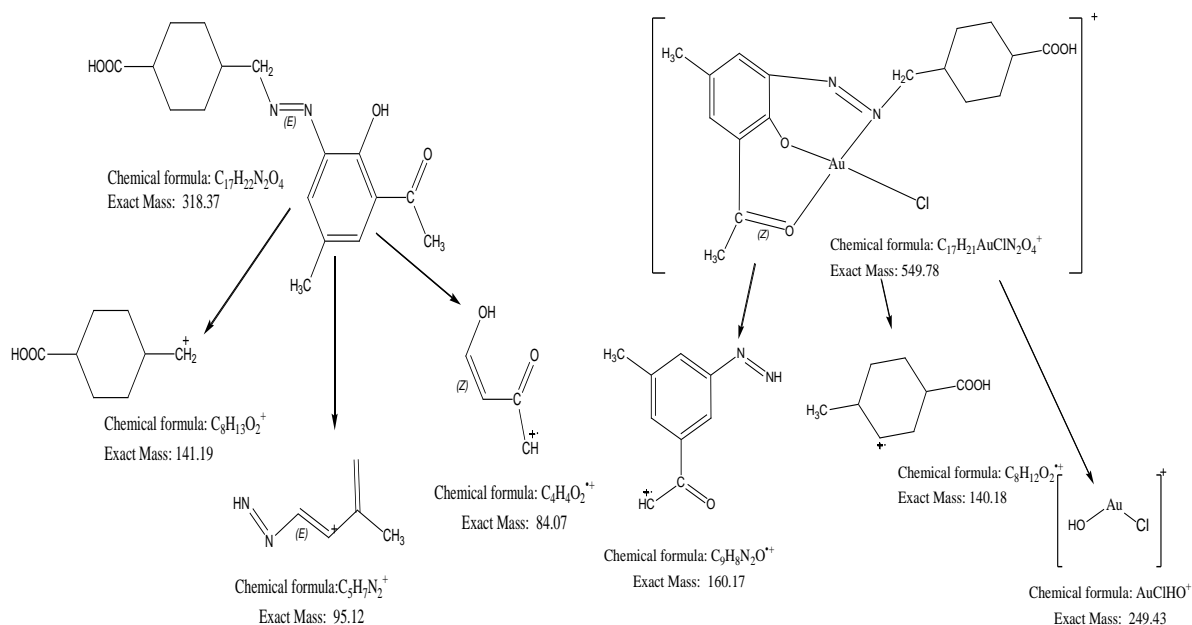
Comp.	λ nm	ν cm^{-1}	ABS	ϵ L. $mol^{-1}cm^{-1}$	Assignment	Λ $S.cm^2$ mol^{-1}	μ_{eff} B.M
[AuLCl]Cl	434 600	23041.47 16666.67	0.53 0.43	530 430	$^1A_{1g} \rightarrow ^1B_{1g}$ $^1A_{1g} \rightarrow ^1A_{2g}$	44.6	dia
[PdLCl]	310 370 500	32258.1 27027.0 20000	1.65 0.99 0.45	1650 990 450	Inter ligand M.L.C.T. $^1A_{1g} \rightarrow ^1B_{1g}$	13.76	dia
[RuL(H ₂ O)Cl ₂]	242 410 499	41322.3 24390.2 20040.1	1.99 0.69 0.67	1990 690 670	Inter ligand MLC.T $^1A_{1g} \rightarrow ^1T_{1g}(G)$	9.21	1.77
[RhL(H ₂ O)Cl ₂]	232 412 499	43103.4 24271.8 20040.1	1.99 0.68 0.6	1990 680 600	Inter ligand ML C.T $^1B_{2g} \rightarrow ^1E_g$	14.8	dia
[PtLCl ₃]	260 310 415	38461.5 32258.1 24096.4	1.8 2.5 0.63	1800 2500 630	Inter ligand M.L.C.T. $^5B_{2g} \rightarrow ^5E_g$	11.42	dia

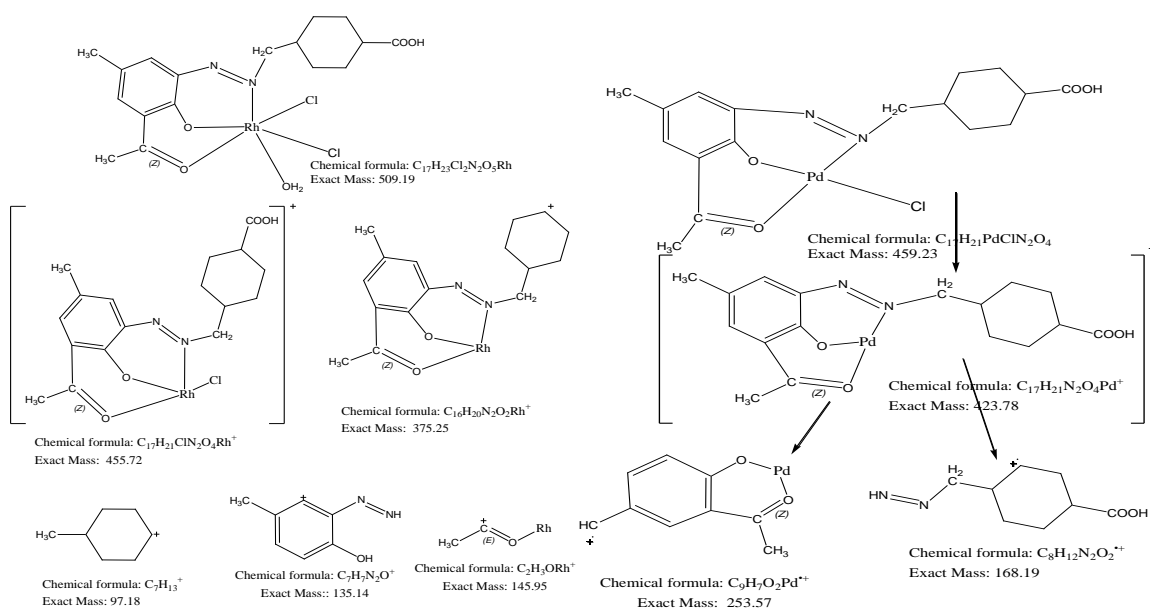
dia= diamagnetic

LC-Mass measurements

The electron impact of fragmentation was used to get the mass spectra of the novel ligand and metal complexes. High-resolution MS was generally used to recover significant fragments linked to breakdown products as well as the free azo ligand and its complexes[26].

In the Figure 7, it can observe that the ligand LH electron impact mass spectrum. The computed molecular weight of this ligand is 318.27 g/mol. A peak at 141.19 m/z in the spectrum was attributed to $C_8H_{13}O_2^+$. The electron impact mass spectrum of the Au+3 complex is shown in Figure 8. Two prominent peaks are evident at m/z values of 95.12 and 84.07. While these could potentially correspond to fragments of the Au+3 complex, their relatively high abundance suggests they may be influenced by other components present as well. The clean nature of the mass spectrum otherwise indicates the complex itself remained intact and stable throughout the ionization and fragmentation processes. The lack of additional peaks reinforces the conclusion that the compound was well-formed and entered the mass spectrometer without decomposing. A peak at 549.78 m/z in the spectra allowed researchers to pinpoint the complex moiety $C_{17}H_{21}AuClN_2O_4^+$. The peaks at 160.17, 140.18, and 249.43 m/z, which are all distinctive, possibly belong to different parts, the mass spectrum of the Pd^{+2} fig. 9 complex displays. The spectra of the complex moiety $C_{17}H_{21}PdClN_2O_4$ revealed a peak at 459.23 m/z that matched the complex moiety. The odd peaks at 253.57 and 168.19 m/z could be the result of other fragments. The structural assignments of the pieces and possible fragmentation routes are provided in Scheme 2[26-29].





Scheme 2: Fragmentation pattern of ligand and its complexes

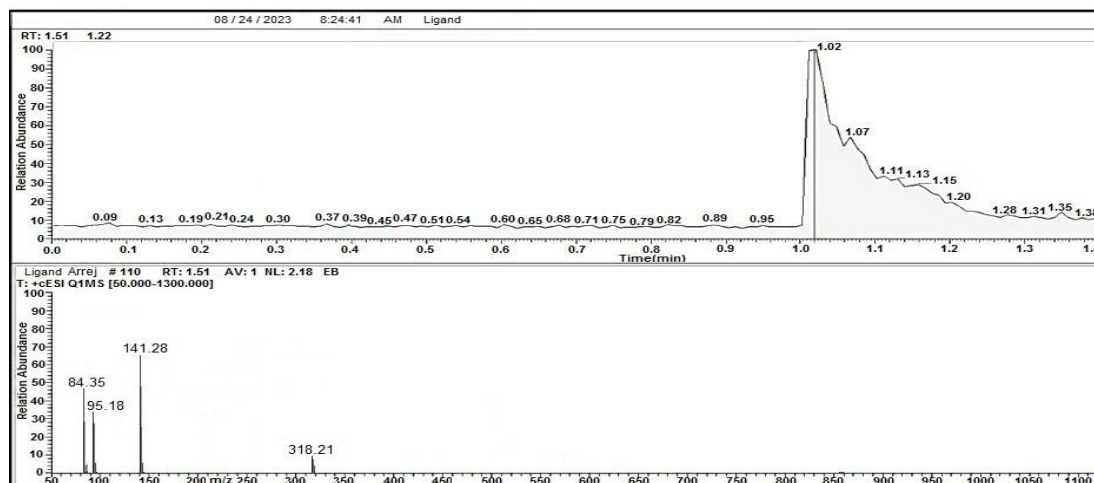


Figure 7: LC-Mass spectrum of ligand

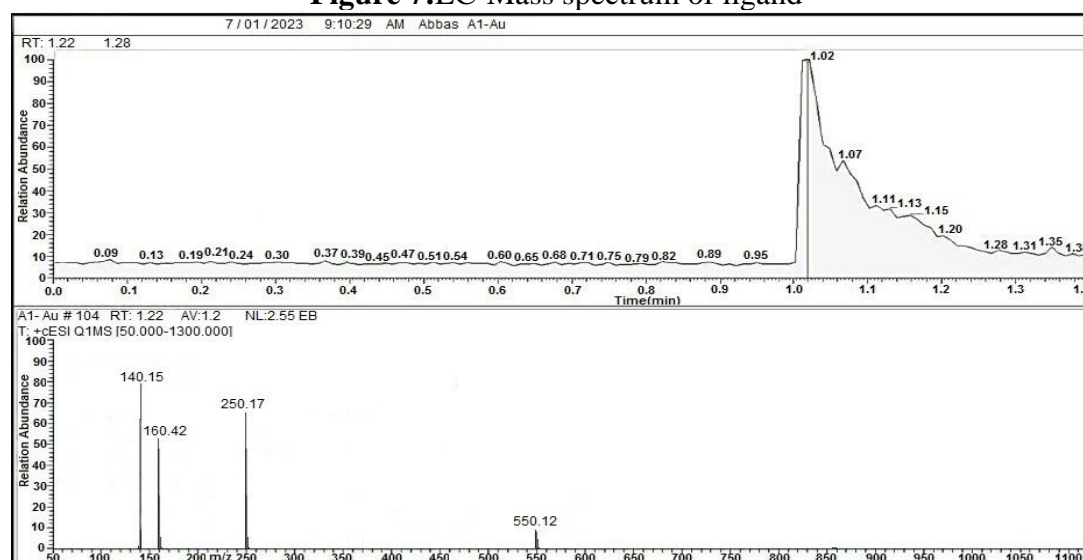


Figure 8: LC-Mass spectrum of Au-complex

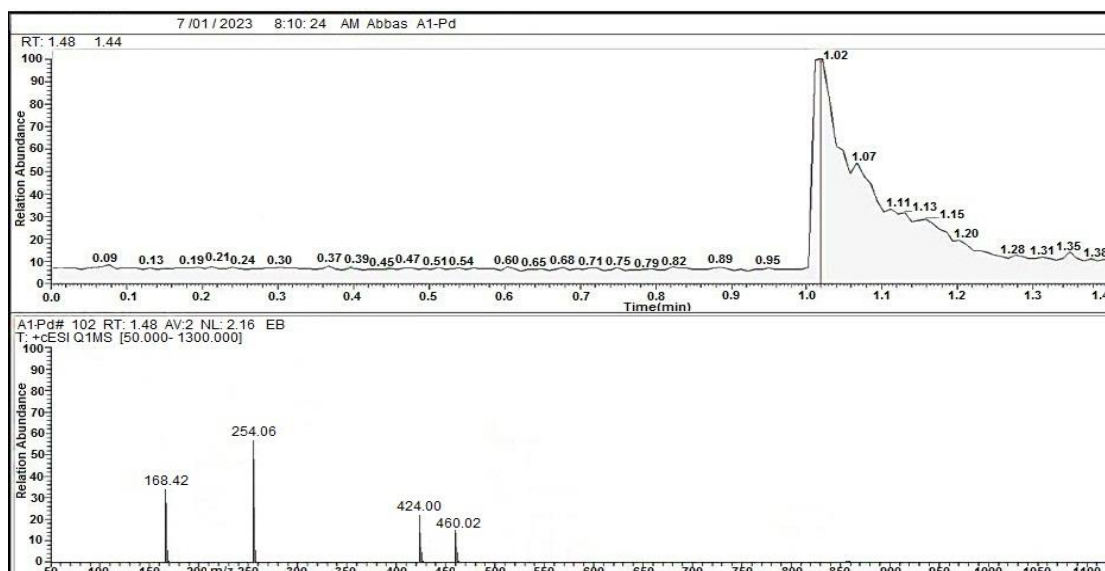
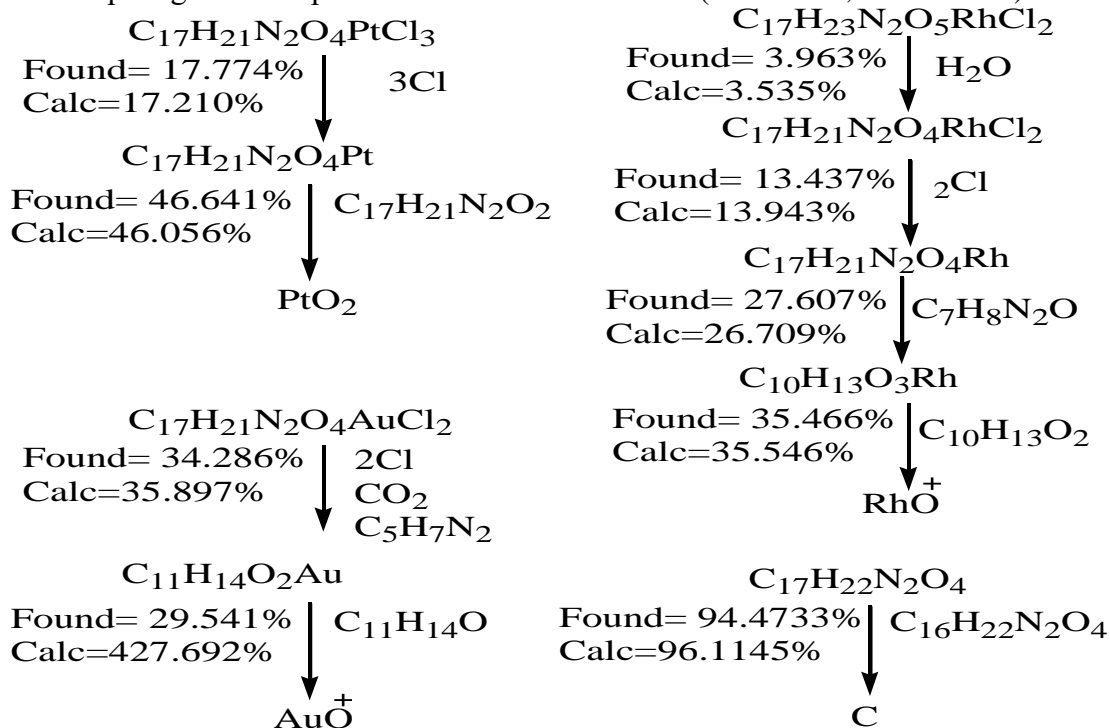


Figure 9: LC-Mass spectrum of Pd- complex

Thermal measurements

The thermal breakdown of the ligand LH and their metal complexes was observed by DSC and TGA, as shown in Figure 10. Information on the thermal deterioration process can be found in Table 4. The produced substances showed a decomposition in the thermogravimetric decomposition curve, with the ligand displaying minimal thermal stability at 111°C and the complexes exhibiting minimal stability at 57°C for Rh, 122°C for Pt and 97°C for Au complexes. The information in Table 4 shows that the ligand decomposes in one degree while leaving a portion intact and that Rh decomposes in four ranges while leaving a residue intact. However, the Pt combination disintegrates with a complete residue in two steps. This corresponds with both the calculated values and the proposed formula [24,26,30]. The DSC curve values for the ligand gave three phases that were endothermic ($\Delta H = -14.2$, -6.3 and 11.0) and Rh complex gave three phases that were endothermic ($\Delta H = -12.5$, -6.8 and 11.5) and Zn complex gave three phases that were endothermic ($\Delta H = -14.2$, -4.0 and 4.1).



Scheme 3: TG decomposition of Ligand and Rh, Pt and Au Complexes

Table 4: TGA data of the ligand HLandsome complexes

Comp.	Step	T _i /°C	T _f /°C	Tmax	Weight mass loss%		Reaction
					Calc	Found	
Ligand	1	111.351	594.515	247.362	96.1145	94.4733	-C ₁₆ H ₂₂ N ₂ O ₄
							C
Calculated: 96.1145 % final=3.8855 %;Estimated 94.4733 % final=5.5267 %							
Rh-complex	1	57.196	168.471	102.431	3.535	3.963	-H ₂ O
	2	168.471	242.1	191.830	13.943	13.437	-2Cl
	3	242.1	389.359	298.12	26.709	27.607	-C ₇ H ₈ N ₂ O
	4	389.359	594.409	416.28	35.546	35.466	-C ₁₀ H ₁₃ O ₂
							RhO ⁺
Calculated:79.733% final =20.267%;Estimated 80.473% final =19.527%							
Pt-complex	1	122.451	309.688	201.820	17.210	17.774	-3Cl
	2	309.688	593.931	413.951	46.056	46.641	-C ₁₇ H ₂₁ N ₂ O ₂
							PtO ₂
Calculated:63.266 % final =36.734 %;Estimated 64.415 % final =35.585%							
Au-complex	1	97.159	330.148	201.820	35.897	34.286	-2Cl,-CO ₂ , -C ₅ H ₇ N ₂
	2	330.148	594.902	413.951	27.692	29.541	-C ₁₁ H ₁₄ O ₂ Au
							AuO ⁺
Calculated:63.589% final =36.411%;Estimated 63.827% final =36.173%							

Antioxidant determination

In the present study, the DPPH assay was employed to evaluate the antioxidant potencies of the target molecules. As shown in Table 5, the percentage inhibition of DPPH radicals is reported for each compound under study. A higher percentage inhibition indicates a greater propensity of that substance to deactivate DPPH radicals through reduction, translating to stronger antioxidant efficacy. These results provide a basis for comparing the relative antioxidant strengths of the various compounds tested here using a validated and routinely performed technique. Better DPPH radical-scavenging effectiveness is indicated by a lower Depress IC₅₀ value. The table clearly shows that almost all of the compounds have effective radical scavenging properties when tested using the DPPH method. It is important to keep in mind that the azo of the complex was more effective as an antioxidant than azo day was see Table 5. The efficiency of DPPH radical scavenging is also impacted by the presence of azoand -OH groups. Additionally, the antioxidant's capabilities are unaffected by the ethylene spacer. As a result, while a check the sample solution is added, the free radical is equalized through the exam sample, which either contributes hydrogen or an electron to result in free radical neutralization. Due to the neutralization of the free radical, the screening sample will produce fewer radicals and the value of IC₅₀, the results are as follow (Ascorbic acid > Au-complex > Pt-complex > Pd-complex > LH > Ru-complex) (see Figure 11)[29-35].

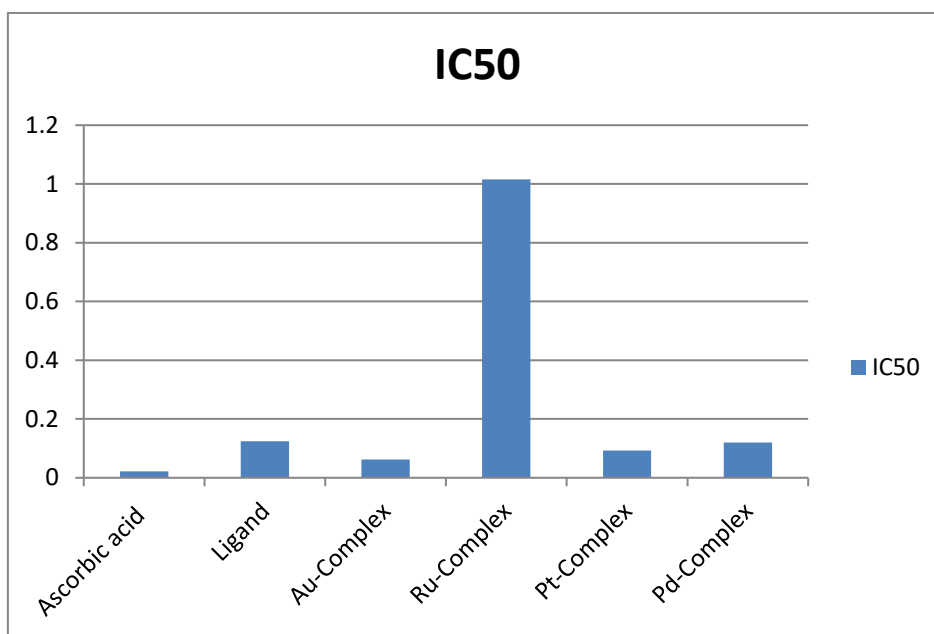


Figure 11: Variations of IC₅₀ values for H₂L ligand and its complexes

Table 4: The antioxidant results of ligand and their metal complexes

Comp.	Conc. Mg/mL	PI	RSA	IC ₅₀ mg/mL
Ligand	0.260	39.26	60.74	0.124
	0.130	43.12	56.88	
	0.065	56.88	43.12	
	0.033	65.76	34.24	
[AuLCl]Cl	0.113	66.87	33.13	0.062
	0.057	71.44	28.56	
	0.028	89.54	10.46	
	0.014	93.98	6.02	
[RuLCl ₂ H ₂ O]	2.083	68.34	31.66	1.015
	1.042	77.65	22.35	
	0.501	82.38	17.62	
	0.296	97.28	2.72	
[PtLCl ₃]	0.260	43.62	56.38	0.093
	0.130	39.26	60.74	
	0.065	43.12	56.88	
	0.033	56.88	43.24	
[PdLCl]	0.326	66.54	33.46	0.120
	0.163	81.38	18.62	
	0.065	96.18	3.82	
	0.033	98.12	1.88	
Ascorbic acid	0.062	15.27	85.19	0.022
	0.031	39.08	62.07	
	0.016	61.07	40.74	
	0.008	74.81	27.41	

Conclusion

Azo compounds are a family of chemicals with clear pharmacological applications and prominence in the literature. Five new chelate complexes with some metallic ions and a novel azo ligand with multiple consistency sites were synthesized. The ligand and its complexes are also being given various methods of characterization. Fourier transform infrared (FT-IR), ^1H & ^{13}C -NMR spectrum characterization, and CHN elemental analysis were employed, *which concentrated on the synthesis of new azo compounds, to validate all of the generated azo compounds*. These substances and their metal complexes exhibited potent antioxidant qualities. Even though combining antioxidant functional groups increases their antioxidant potential, it is still necessary to investigate the antioxidant characteristics of those that have already been created and to create new antioxidant functional group complexes with additional qualities.

References

- [1] H.S. Mohammed, H.A. Al-Hasan, Z. Chaieb, Z. Zizi, H.N. Abed. "Synthesis, characterization, DFT calculations and biological evaluation of azo dye ligand containing 1, 3-dimethylxanthine and its Co (II), Cu (II) and Zn (II) complexe", *Bulletin of the Chemical Society of Ethiopia*, vol 37, no. 2, pp. 347-56, 2023.
- [2] G. G. Mohamd, W. H. Mahmoud and A. M. Refaat, "Nano-Azo Ligand and Its Superhydrophobic Complexes: Synthesis, Characterization, DFT, Contact Angle, Molecular Docking, and Antimicrobial Studies", *Journal of Chemistry*, vol. 2020, pp. 1-9, 2020.
- [3] H. M. Alabidi, M. A. Alabidi and N. F. Makki, " Synthesis and Spectroscopic Studying of New Azo Ligand From 2-Naphthol Derivative and Its Complexes with Some Transition Metal Ions," *AL-Qadisiyah Journal of pure Science*, vol. 23, no. 1, pp. 186-195, 2018.
- [4] I. H. Ibraheem, N. S. Mubder, M. M. Abdullah, H. Al-Neshmi, "Synthesis, characterization and bioactivity Study from azo-ligand derived from methyl-2-amino benzoate with some metal ions", *Baghdad Science Journal*, vol. 20, no. 1, pp. 0114-0114, 2023.
- [5] S. M. Reda and A. A. S. Al-Hamdani, "Mn (II), Fe (III), Co (II) and Rh (III) complexes with azo ligand: Synthesis, characterization, thermal analysis and bioactivity", *Baghdad Science Journal*, vol 20, no.3, pp .0642-0660, 2023.
- [6] M. Y. Dhamra, "Spectrophotometric Determination of Tranexamic Acid by Azo-Dye Formation Application to Pharmaceutical Preparations", *Journal of Education and Science*, vol. 24, no. 3, pp. 21-33, 2011
- [7] H. A. Kyhoiesh, K.J. Al-Adilee, "Synthesis, spectral characterization, antimicrobial evaluation studies and cytotoxic activity of some transition metal complexes with tridentate (N, N, O) donor azo dye ligand", *Results in chemistry*, vol.1, no3, pp.100245, 2021.
- [8] Y.J. Sahar, H Mohammed, Z.N. Al-Abady, "Synthesis and characterization of new metal complexes containing azo-indole moiety and anti-leukemia human (HL-60) study of its palladium (II) complex ", *Results in Chemistry*, vol. 1, no.1, pp. 100847, 2023.
- [9] N. Nagasundaram, C. Govindhan, S. Sumitha, N. Sedhu, K. Raguvaran, S. Santhosh, A. Lalitha, "Synthesis, characterization and biological evaluation of novel azo fused 2, 3-dihydro-1H-perimidine derivatives: In vitro antibacterial, antibiofilm, anti-quorum sensing, DFT, in silico ADME and Molecular docking studies," *Journal of Molecular Structure*, vol.1248, pp. 131437, 2022.
- [10] A. A. El-Habeeb and M. S. Refat, " Synthesis, structure interpretation, antimicrobial and anticancer studies of tranexamic acid complexes towards Ga (III), W(VI), Y(III) and Si (IV) metal ions" , *Journal of Molecular Structure*, vol. 2019, no. 1175, pp. 65-72, 2019.
- [11] M. Lashanizadegan, H A Ashari, M. Sarkheil, M. Anafcheh, S. Jahangiry, "New Cu (II), Co (II) and Ni (II) azo-Schiff base complexes: Synthesis, characterization, catalytic oxidation of alkenes and DFT study", *Polyhedron*, vol. 15, pp.20, 2021.
- [12] J. Keshavayya, I. Pushpavathi, C. T. Keerthikumar, M. R. Maliyappa, B. N. Ravi, "Synthesis, characterization, computational and biological studies of nitrothiazole incorporated heterocyclic azo dyes", *Structural Chemistry*, vol.31 ,no.4, pp.1317-1329, 2020.

- [13] M. Kaur, S Kumar, SA Younis, M Yusuf, J Lee, S Weon, KH Kim, AK Malik, "Post-Synthesis modification of metal-organic frameworks using Schiff base complexes for various catalytic applications", *Chemical Engineering Journal*, vol.423, pp.130230, 2021.
- [14] H. S. Mandour, S.A. Abouel-Enein, R. M. Morsi, L. A. Khorshed, "Azo ligand as new corrosion inhibitor for copper metal: Spectral, thermal studies and electrical conductivity of its novel transition metal complexes," *Journal of Molecular Structure*, vol.5, no.1225, pp.129-159, 2021.
- [15] R.K.H. Al-Daffaay, "Preparation-and Spectroscopic Characterization of Transition Metal Complexes with Schiff base 2-[1-(1H-indol-3-yl)ethylimino) methyl]naphthalene-1-ol", *Baghdad Science Journal*, vol. 19, no. 5, pp. 1036-1044.
- [16] A. M. A. Al-Khazraji and R. A. M. Al Hassani, "Synthesis, Characterization and Spectroscopic Study of New Metal Complexes form Heterocyclic Compounds for Photostability Study", *Systematic Reviews in Pharmacy*, vol. 11, no. 5, pp. 535-555, 2020.
- [17] R. M. Silverstein, G. C. Bassler and T. C. Movril, "*Spectroscopic Identification of Organic Compounds*", Wiley: New York, 1981, ed4.
- [18] I.S. Hamza, W.A. Mahmmoud, A.A. Al-Hamdani, S.D. Ahmed, A.W. Allaf, W. Al Zoubi, "Synthesis, characterization, and bioactivity of several metalcomplexes of(4-Amino-N-(5-methylisaxazol-3-yl)-benzene sulfonamide)", *Inorganic Chemistry Communications*, vol 144, 109776, pp. 1-23, 2022.
- [19] M.A Hadi, I.K. Kareem, "synthesis, Characterization and Spectral Studies of a new Azo-Schiff base Ligand Derived from 3, 4-diamino benzophenone and its Complexes with Selected Metal Ions", *Research Journal Advanced Sci.*, vol 1, no. 1, pp. 54-73, 2020.
- [20] K. Nakamoto, "*Infrared and Raman Spectra of Inorganic and Coordination Compounds*", Wiley Inter Science: New York. 1997.
- [21] A. B. P. Lever, "*Inorganic Electronic Spectroscopy*", Elsevier Publishing Company: Amsterdam, London, 1968, pp. 121, ed6.
- [22] J. Keshavayya, I. Pushpavathi, C. T. Keerthikumar, M. R. Maliyappa, B. N. Ravi, "Synthesis, characterization, computational and biological studies of nitrothiazole incorporated heterocyclic azo dyes", *Journal Struct. Chemistry*, vol. 31, no. 4, pp.1317-1329, 2020.
- [23] WJ. Geary, "The use of conductivity measurements in organic solvents for the characterisation of coordination compounds", *Coordination Chemistry Reviews*, vol., 7, no. 1, pp. 81–122, 1971.
- [24] G. D. Reem, H. M. Walaa and G. M. Gehad, "Metal complexes of tetradentateazo-dye ligand derived from 4,4-oxydianiline: Preparation, structural investigation, biological evaluation and MOE studies", *Applied Organometallic Chemistry*, vol. 34, no. 10, pp. 1-20, 2020.
- [25] N.Shaalan, "Preparation, Spectroscopy, Biological Activities and Thermodynamic Studies of New Complexes of Some Metal Ions with 2-[5-(2-Hydroxy-Phenyl)-1, 3, 4-Thiadiazol-2-Ylimino]-Methyl-Naphthalen-1-Ol]", *Baghdad Science Journal*, vol. 19, no. 4, pp. 0829, 2022.
- [26] H.S. Mohammed, "Synthesis and Characterization of Some Complexes of Azo-Chalcone Ligand and Assessment of their Biological Activity", *Materiale Plastice*, vol. 58, no.3, p. 23-31, 2021.
- [27] O. Ozdemir, "Bis-azo-linkage Schiff bases—Part (II): Synthesis, characterization, photoluminescence and DPPH radical scavenging properties of their novel luminescent mononuclear Zn (II) complexes", *Journal of Photochemistry and Photobiology A: Chemistry*, vol. 392, pp. 112356, 2020.
- [28] N. Asim, MH Amin, MA Alghoul, SN Sulaiman, H Razali, M Akhtaruzzaman, N Amin, K Sopian, "Developing of chemically treated waste biomass adsorbent for dye removal", *Journal Natural Fibers*, vol.8, no. 7, p. 968-977, 2021.
- [29] S.A. Jaber, HA Kyhoiesh, SH Jawad, "Synthesis, characterization and biological activity studies of cadmium (II) complex derived from azo ligand 2-[2-(5-bromo Thiazolyl) azo]-5-dimethyl amino benzoic acid", *In Journal of Physics: Conference Series*, vol. 1818, no1, pp. 012013, 2021.
- [30] M. Hasan, "Synthesis, Identification, and Biological Study for Some Complexes of Azo Dye Having Theophylline", *The Scientific World Journal*, vol. 2021, pp. 1-9, 2021.
- [31] R.R. Ali, H.S. Mohammed, "Synthesis and characterization and biological study of pyridylazo ligand and its compounds of Co, Ni and Cu divalent ions", *In Journal of Physics: Conference Series*, vol. 1999, No. 1, pp. 012009, 2021.
- [32] A. Rananaware, M. Samanta, R. S. Bhosale, "Photomodulation of fluoride ion binding through anion- π interactions using a photoswitchable azobenzene system", *Scientific Reports*, vol. 8, no. 1, pp. 1-10, 2016.

- [33] A.N. Alhakimi, MM Shakhdofo, S Saeed, AM Shakhdofo, MS Al-Fakeh, AM Abdu, IA Alhagri, "Transition Metal Complexes Derived from 2-hydroxy-4-(p-tolyldiazenyl) benzylidene)-2-(p-tolylamino) acetohydrazide Synthesis, Structural Characterization, and Biological Activities", *Journal Korean Chemical Soc.*, vol. 65, no. 2, pp. 93-105, 2021.
- [34] B. Vhanale, D. Kadam, A. Shinde, "Synthesis, spectral studies, antioxidant and antibacterial evaluation of aromatic nitro and halogenated tetradentate Schiff bases", *Heliyon*, vol. 8, no. 2022, pp. 1-7, 2022.
- [35] M.D. Ashrafzaman, F.K. Camellia, A. Al-Mahmud, J.M.D. Pramanik, K. Nahar, M.D.M. Haque and M.D. Kudrat-E-Zahan, "Bioactive Mixed Ligand Metal Complexes Of Cu(II), Ni(II), And Zn(II) Ions: Synthesis, Characterization, Antimicrobial And Antioxidant Properties", *Journal of the Chilean Chemical Society*, vol. 66, no. 3, pp. 5295-5299, 2021.